

Article

Creating Values from Biomass Pyrolysis in Sweden: Co-Production of H₂, Biocarbon and Bio-Oil

Ilman Nuran Zaini ^{1,*} , Nanta Sophonrat ^{1,2} , Kurt Sjöblom ² and Weihong Yang ^{1,2}

¹ Department of Material Sciences and Engineering, KTH Royal Institute of Technology, Brinellvägen 23, 11428 Stockholm, Sweden; nanta.sophonrat@envigas.com (N.S.); weihong@kth.se (W.Y.)

² Envigas AB, Industrivägen 53, 93252 Bureå, Sweden; kurt.sjoblom@envigas.com

* Correspondence: zaini@kth.se

Abstract: Hydrogen and biocarbon are important materials for the future fossil-free metallurgical industries in Sweden; thus, it is interesting to investigate the process that can simultaneously produce both. Process simulations of biomass pyrolysis coupled with steam reforming and water-gas-shift to produce H₂, biocarbon, and bio-oil are investigated in this work. The process simulation is performed based on a biomass pyrolysis plant currently operating in Sweden. Two co-production schemes are proposed: (1) production of biocarbon and H₂, and (2) production of biocarbon, H₂, and bio-oil. Sensitivity analysis is also performed to investigate the performance of the production schemes under different operating parameters. The results indicated that there are no notable differences in terms of the thermal efficiency for both cases. Varying the bio-oil condenser temperature only slightly changes the system's thermal efficiency by less than 2%. On the other hand, an increase in biomass moisture content from 7 to 14 wt.% can decrease the system's efficiency from 79.0% to 72.6%. Operating expenses are evaluated to elucidate the economics of 3 different cases: (1) no bio-oil production, (2) bio-oil production with the condenser at 50 °C, and (3) bio-oil production with the condenser at 130 °C. Based on operation expenses (OPEX) and revenue alone, it is found that producing more bio-oil helps improving the economics of the process. However, capital costs and the cost for post-processing of bio-oil should also be considered in the future. The estimated minimum selling price for biocarbon based on OPEX alone is approx. 10 SEK, which is within the range of the current commercial price of charcoal and coke.

Keywords: process simulation; bioenergy; hydrogen production; biochar; Aspen plus; techno-economic analysis



Citation: Zaini, I.N.; Sophonrat, N.; Sjöblom, K.; Yang, W. Creating Values from Biomass Pyrolysis in Sweden: Co-Production of H₂, Biocarbon and Bio-Oil. *Processes* **2021**, *9*, 415. <https://doi.org/10.3390/pr9030415>

Academic Editor: Juan Francisco García Martín

Received: 11 January 2021

Accepted: 20 February 2021

Published: 25 February 2021

Publisher's Note: MDPI stays neutral with regard to jurisdictional claims in published maps and institutional affiliations.



Copyright: © 2021 by the authors. Licensee MDPI, Basel, Switzerland. This article is an open access article distributed under the terms and conditions of the Creative Commons Attribution (CC BY) license (<https://creativecommons.org/licenses/by/4.0/>).

1. Introduction

Metal production is one of the main industries highly dependent on fossil fuels and emitting a large amount of CO₂. In 2019, Sweden produced 29 million tons of iron [1] which resulted in approximately 57 million tons of CO₂ emission (1.97 ton CO₂/ton steel) [2]. A significant part of CO₂ comes from coal, coke, oil, and natural gas used in steel production processes including sintering, coke making and blast furnace [3]. Blast furnaces, which account for the largest CO₂ emission in the steel plant, approximately consume 250–300 kg of coke per ton hot metal produced [4]. Some of the methods to reduce CO₂ emission from metallurgical processes are to apply new technologies and to use renewable fuels. This includes the use of H₂ as a reduction agent instead of coke (HYBRIT project [5]) and the replacement of coal and coke with biocarbon/charcoal from biomass [6].

Sweden has abundant forest resources as their forest accounts for 57% of the total land area [7]. Forest industry in Sweden is well managed with about 120 and 90 million cubic meters of the forest grew and felled every year [7]. In 2020, it was estimated that the Swedish productive forest could provide a total energy of about 450 TWh/year, which is significantly higher than the total energy demand in Sweden (370 TWh/year) [8]. The main forest industries are timber production for furniture and construction, and the pulp and

paper industry. The availability of forest and forest residue and the demand for renewable fuels for Swedish metallurgical industries provide a good incentive for turning biomass into biocarbon and renewable H₂.

The main process for biocarbon production is pyrolysis of biomass [3,9] which is the application of heat to a feedstock in the absence of oxygen. Some specific properties are required to produce biocarbon for metallurgical processes, including high fixed carbon content, low moisture/volatile content, low CO₂ reactivity, and high mechanical strength [3,10]. The pyrolysis process parameters must be adjusted to achieve these required properties [9]. In the pyrolysis process, pyrolysis vapor which consists of bio-oil and gas is also produced. This vapor could be upgraded/reformed to produce H₂ [11]. Although there are many processes for producing renewable H₂ such as the electrolysis of water [12], biomass/waste steam gasification [13,14], and supercritical water gasification [15], H₂ production via the upgrading of pyrolysis vapor presents a very attractive option [11] as H₂ is co-produced together with biocarbon, and the reforming process can be adjusted independently of the pyrolysis process. The process also has a potential to be appended to the already existing large scale pyrolysis plant. Besides in-line reforming of pyrolysis vapor, H₂ can also be produced via pyrolysis by catalytic steam reforming of bio-oil or its fractions [16,17], and pyrolysis using biochar as an in situ catalyst to promote H₂ formation [18].

Table 1 summarizes previous experimental works of woody biomass pyrolysis processes with in-line pyrolysis vapor reforming for H₂ production. These works include catalytic upgrading of pyrolysis vapor [19,20] and catalytic steam reforming of pyrolysis vapor [21–24]. Pyrolysis temperature is in the range of 500–750 °C, while the catalytic steam reformer temperature is in the range of 600–900 °C. In most cases, Ni-based catalyst is employed together with steam to biomass ratio (S/B) of 4. The highest H₂ yield is around 10–11 wt.% which is close to the maximum theoretical yield based on steam reforming of pyrolysis vapor of around 11 wt.% of dry biomass (depending on the elemental analysis of different biomasses). This result is achieved when the liquid/bio-oil is fully converted as in [21,24]. As shown in Table 1, when the vapor is not fully converted, bio-oil could be produced, and a high CO concentration is observed. The CO content can be further converted to H₂ via the water-gas shift (WGS) reaction by adding more steam [11]. It should be noted that catalyst deactivation could also be a problem during an operation as in [21] where deactivation occurs after 1 h of operation. This will be further discussed in the next section when we consider process schemes.

Table 1. Biomass pyrolysis with in-line reforming of pyrolysis vapor for H₂ production.

Configuration and Operating Parameters	Pyrolysis Reactor/Steam Reforming Reactor	Catalyst	H ₂ Yield (wt.%)	H ₂ Concentration (vol.%)	CO Concentration after Reformer (vol.%)	Liquid Yield (wt.%)	Ref.
Wood sawdust, Pyrolysis (500 °C) + steam reformer (600 °C, 20 g _{cat} min/g _{volatile} , S/B = 4 (S/C~8))	Spouted bed/fluidized bed, Lab-scale	Ni commercial	11	66 (94% of stoic)	3	0 (100% conversion) ¹	[21]
Wood sawdust, Pyrolysis (500 °C) + steam reformer (800 °C, S/B ~4)	Fixed bed/fixed bed, Lab-scale	Ni/CaAlO _x	2.8	45	44	1–5	[22]
Wood pellet, Pyrolysis (500 °C) + steam reformer (760 °C, S/B = NA)	Screw reactor/fixed bed, Bench-scale	NiO/Al ₂ O ₃		44	30	27	[23]
Wood chip, Pyrolysis (600 °C) + steam reformer (650 °C, S/C=3)	Fluidized bed/fixed bed, Lab-scale	Ni/Al ₂ O ₃ , Ni-brown coal char	Approx. 10	60	Approx. 10	<1	[24]
Olive tree cuttings, Pyrolysis (750 °C) + catalytic reactor (900 °C, no additional steam)	Non-stirred batch/fixed bed, Lab-scale	Biochar + Ni/Al ₂ O ₃ -CeO ₂		17.6	47.4	33.8	[19, 20]

¹ Catalyst deactivation occurs after 1 h of operation, and the conversion drops to ~50% after 1.5 h of operation [25]. S/B = steam to biomass ratio by weight, S/C = molar ratio of steam to carbon in volatiles fed into the reformer.

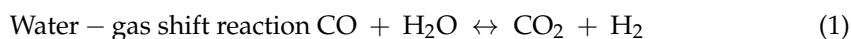
Considering the review above, the application of pyrolysis for co-production of biocarbon and H₂ is beneficial since both products are necessary for future metallurgical processes. Therefore, further investigation of this process based on its energy efficiency and economy aspect is crucial for process design. Process simulation is an important tool for feasibility evaluation and process design. To the best of the authors' knowledge, process simulations investigating co-production of biocarbon and H₂ via biomass pyrolysis and subsequent vapor upgrading are rarely available in the literature. The following literature is some related works. Situmorang et al. [26] reported a process simulation to produce H₂ from pyrolysis vapor via steam reforming combined with biochar gasification using chemical looping. Jones et al. [27] reported a process design to convert biomass into hydrocarbon fuels. Fast pyrolysis was employed with char combustion to supply energy to the process. A part of the process gas was converted to H₂ by steam reforming of C₂₊ compounds. Larsson et al. [28] performed a process simulation of slow pyrolysis to produce biochar and CH₄.

In this study, different co-production scenarios of biocarbon, hydrogen, and bio-oil based on the biomass pyrolysis process are technically evaluated employing process simulation. Furthermore, preliminary operation expense (OPEX) of each scenario are calculated to find the strategy that offers the most economic benefit. The economic calculation is carried out within the scope of Sweden.

2. Materials and Methods

2.1. Process Description of the Proposed Co-Production Systems

In this study, an intermediate pyrolysis process with electrically heated screw reactor is chosen in the simulation to resemble Envigas pyrolysis process for biocarbon production. The pyrolysis vapor is then reformed in an electrically heated reformer and converted to H₂ through a WGS reaction (Equation (1)) in a WGS reactor. The output gas is then separated using pressure swing absorption (PSA).



According to Table 1, most of the H₂ production process from pyrolysis vapor only used one reformer which serves as a reactor for steam reforming. Most of the previous works were done on lab-scale, which did not incorporate WGS reactors [11]. However, on a pilot or an industrial process, WGS reactors might be necessary to increase the yield and purity of hydrogen stream according to Equation (1). To assess the necessity of having WGS reactors, the amount of CO at the steam reformer outlet should be known. If the CO level is high, the WGS reactor is required. Table 1 shows that the range of CO vol% after steam reformer is very wide due to the different catalysts and operating conditions. Therefore, a WGS reactor is added to our proposed process.

Another vital operation issue is the deactivation of the catalyst. Due to the high concentration of bio-oil vapor compared to natural gas stream and low temperature for steam reforming (600 °C), catalyst deactivation in the steam reforming process occurs quickly, e.g., within 1 hr. in a lab-scale test [29]. Deactivation can be slowed down using a calcined dolomite guard catalyst bed before the Ni-catalyst bed [30,31]. Steam is added to the guard bed kept at higher than 800 °C to allow thermal cracking and steam gasification. The less complicated gas/vapor stream is then fed to Ni-catalyst bed. It seems that carbon deposition occurs in dolomite guard bed to some extent, and a regeneration process of guard bed was performed by treatment with pure steam at 800 °C for 30 min [30].

Some works suggest removing pyrolytic lignin fraction from bio-oil before steam reforming to slow down catalyst deactivation. Some methods for in-line removal of this fraction are (1) fractional condensation [32], and (2) thermal treatment [33]. Fractional condensation removes pyrolytic lignin and other heavy compounds in bio-oil as a liquid. On the other hand, thermal treatment turns pyrolytic lignin fraction into coke, which is then removed from the system.

From the above literature reviews, we proposed to investigate two co-production schemes as follow:

Scheme 1: to produce biocarbon with H₂. As shown in Figure 1, the whole pyrolysis vapor will be used for hydrogen production. One steam reformer unit is used to model the dolomite guard bed and the Ni-catalyst bed with a thermodynamic equilibrium model.

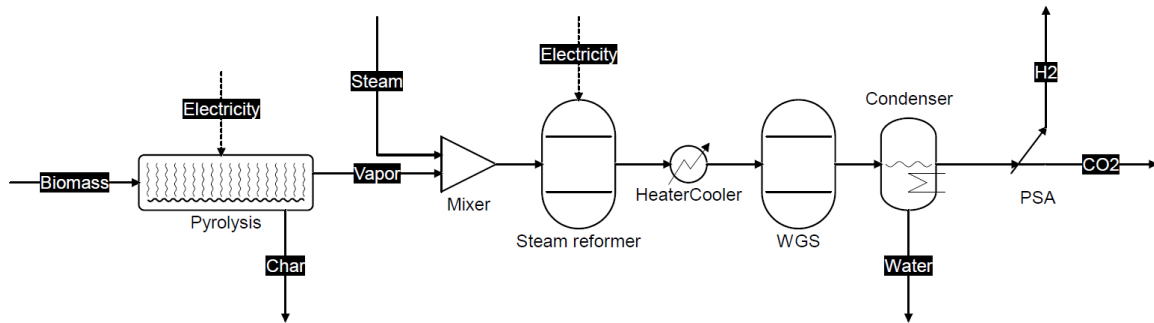


Figure 1. Scheme 1: production of H₂ and biocarbon.

Scheme 2: to produce biocarbon with bio-oil and H₂. As shown in Figure 2, fractional condensation will be applied to condense heavy fraction of bio-oil. The light fraction of bio-oil will be used for H₂ production.

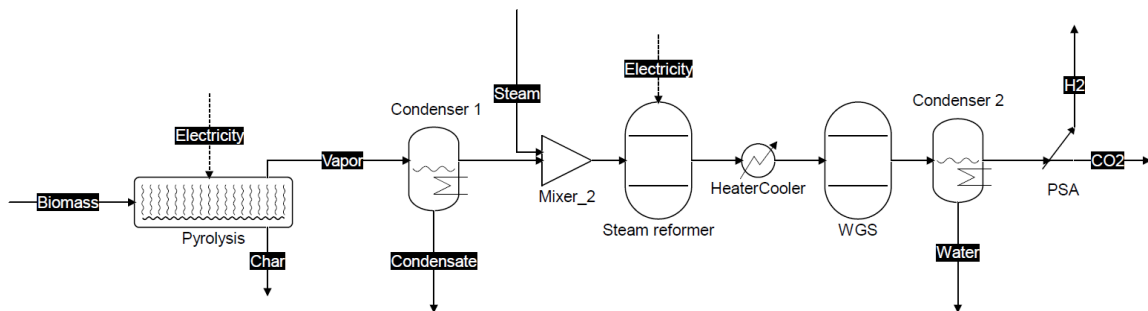


Figure 2. Scheme 2: production of H₂, bio-oil, and biocarbon.

2.2. Materials and Products Analysis

The elemental analysis of raw biomass and char from the Envigas biocarbon pilot plant in Bureå, Sweden, was performed by an external laboratory (Eurofins, Sweden) following ASTM-D5373:2016 and ASTM-D5142:2009 standards. The typical standard deviation of the analysis is 5–10% as reported by the external laboratory. The results are shown in Table 2. Unfortunately, bio-oil and gas were not analyzed. Therefore, their compositions and yields are obtained by using assumptions from literature and elemental balance.

Table 2. Properties of raw biomass and char.

		Biomass	Char
Moisture	wt.%, as *	6.6	<2
Ash	wt.%, as	0.24	1.2
C	wt.%, daf **	51.7 ± 2.6	
H	wt.%, daf	6.18 ± 0.62	
O #	wt.%, daf	42.12 ± 2.66	
C	wt.%, waf †		95.24 ± 4.76
H	wt.%, waf		1.32 ± 0.13
O #	wt.%, waf		3.44 ± 4.76

Table 2. Cont.

		Biomass	Char
LHV	MJ/kg, af	19.1 ± 1.0	34.5 ± 1.7
Heat of formation †	MJ/kg	−5.274	1.688
Heat capacity	J/kgK	1190 [34]	1300 [35]

calculated from 100-C-H, * as = as received, ** daf = dry ash-free basis, † waf = wet ash-free basis, ‡ Calculated based on LHV.

2.3. Calculation/Simulation

The process simulations conducted in this study are carried out using the Aspen Plus version 9.0 (Aspen Technology, Inc., Bedford, MA, USA) process simulation package. The simulations are performed under the following general conditions and assumptions:

- The biomass feed input is 1000 kg/h.
- The process is operated under steady-state conditions.
- Gases are treated as ideal gases, and the ambient pressure is 101.325 kPa.
- The property method selected is Peng-Robinson for the all-reactor modules.
- The efficiency of the compressor and pump are 90 and 75%, respectively [36].

The minimum temperature approach (ΔT_{min}) of heat exchangers is 10 °C [36].

The pyrolysis mass and energy balance are obtained from the pilot plant operation at Envigas. The data is then used as an input for the remaining downstream processes in the Aspen Plus.

2.4. Assumptions and Basis for Calculations

2.4.1. Pyrolysis Yields

Figure 3 shows a pyrolysis process at Envigas biocarbon pilot plant in Bureå, Sweden. An intermediate pyrolysis process of 100 kg/h biomass was performed in an electrically heated screw reactor with the pyrolysis temperature of 550–650 °C. The char (biocarbon) yield is obtained directly from the process by recording weights of the feedstock and the produced biocarbon. The char yield is 23.0 ± 2.5 wt.%. Liquid and gas yields are rounded values from a reference [19] in the case of pyrolysis without any catalyst. The pyrolysis yields are given in Equations (2) and (3).

$$100 \text{ wt.\% Biomass} \rightarrow 6.6\text{wt.\% Moisture} + 0.24 \text{ wt.\% Ash} + 93.16\text{wt.\%Biomass (daf)} \quad (2)$$

$$100 \text{ wt.\% Biomass (daf)} \rightarrow 23\text{wt.\% Char} + 43\text{wt.\% Bio - oil} + 34\text{wt.\%Gas} \quad (3)$$

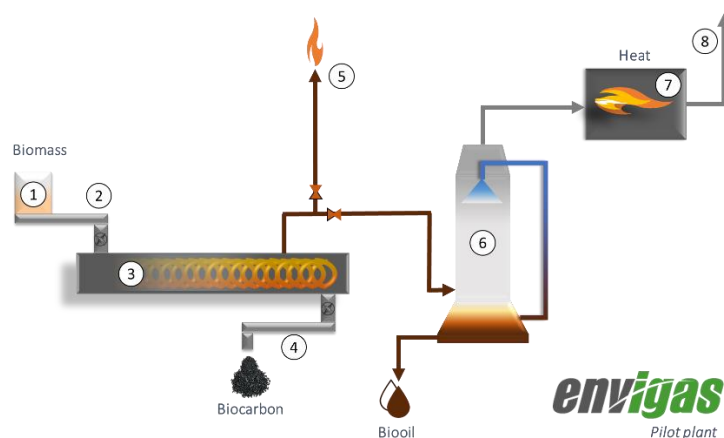


Figure 3. Envigas pilot plant process for biocarbon production: (1) biomass storage, (2) dosing screw, (3) electrically heated pyrolysis screw reactor, (4) char cooling screw, (5) emergency flare, (6) condenser, (7) off-gas burner, (8) exhaust pipe.

2.4.2. Liquid and Gas Compositions

Pyrolysis vapor consists of bio-oil and non-condensable gases. Elemental compositions of pyrolysis vapor are calculated via the difference of those of biomass and char. The composition of liquid given in Table 3 is based on middle values from a literature [37]. As for intermediate pyrolysis, the water content in bio-oil is usually in the range of 40–60 wt.% [38]. Considering the moisture content in the raw feedstock of 6.6 wt.% (Table 2) and the yield of bio-oil of 43 wt.% of dry biomass (Equation (3)), the calculated water content of bio-oil (dry biomass basis) of 35 wt.% will give the final moisture content in bio-oil (wet biomass basis) of approx. 41 wt.%, according to the range in the literature [37]. The high molecular weight lignin and hybrid oligomer (HMWLIG) represents a lump of all heavy compounds from pyrolytic lignin, hybrid oligomers and humins. Its elemental composition (Table 5) is calculated by the elemental balance of the pyrolysis products and the feedstock, given that the H/C ratio is less than 2. In the Aspen Plus, the HMWLIG is represented by a non-conventional solid compound.

Table 3. Pyrolysis liquid compositions used in this work.

Compounds	Ref. [37]	Values Used in This Study (wt.% of Bio-Oil)
Water	(19–30 wt.%)	35
C2-C4 light molecules	(10–22 wt.%)	
Acetic acid	2–6	2
Hydroxyacetaldehyde	1–14	7
Hydroxyacetone (Acetol)	5–9	7
Formic acid	<1	
2-Butenoic acid		2
Monofurans	(1 wt.%)	
Furfural	0.1–0.2	1
2(5H)-Furanone	0.2–0.8	
Monophenols	(1–5 wt.%)	
Phenol	0.1	
Guaiacol	0.2–0.5	
Cresol	0.1–0.4	1
Syringol	0.4	
Isoeugenol	0.1–0.2	1
Anhydrosugar	(10–20 wt.%)	
Levoglucofan	NA	10
Cellobiosan	NA	
Maltose		10
Pyrolytic lignin	(15–27 wt.%)	
Hybrid oligomers	(11–18 wt.%)	
Humins	(3–7 wt.%)	
High molecular weight lignin and hybrid oligomers (HMWLIG)		24
Total		100

The balance H is added to H₂ gas. Since the reformer is simulated using Gibbs reactor, the final H₂ content will not be affected by this initial adjustment. The gas composition shown in Table 4 is based on rounded values from reference [39]. The gas composition was adjusted to achieved elemental balance.

Table 4. Pyrolysis gas composition used in the simulation.

Gas Compositions	wt. %
H ₂	1.2
CO	45.00
CO ₂	35.00
CH ₄	12.00
C ₂ H ₆	2.00
C ₃ H ₈	4.80

Table 5. Properties of the high molecular weight lignin-derived compounds (HMWLIG).

High MW Lignin-Derived Compound	wt. %	Formula (mol)
C	67.1	20
H	11.0	38.935
O	21.9	4.913
LHV *	MJ/kg	33.25
Heat of formation †	MJ/kg	−6.72
Heat capacity ‡	J/kgK	1970 [40]

* Calculate using Dulong formula for HHV; † Calculate from LHV. ‡ From the reference of bio-oil with 10 wt.% moisture, calculate for the dry basis.

2.4.3. Bio-Oil Condenser

In Scheme 2, the hot vapor products are directly condensed to collect bio-oil before the steam reforming process. In Envigas pilot plant, the condenser system consists of a scrubber that can be operated at different temperatures (see Figure 3). As seen in Figure 4b, the condenser system can be modeled by using a flash block module (“COND”) in Aspen Plus. The composition and mass flow of the “PYRO1” stream coming into the flash block is defined based on the pyrolysis yield calculation, as explained in the previous section. In this study, the condenser temperature is varied within the range of 50–130 °C. The HMWLIG in the pyrolysis vapor is assumed to fully condense into “BIO-OIL” stream for all operating temperatures. Although the rest of the fraction condenses differently based on the operating temperature.

On the other hand, no “COND” block is required for Scheme 1 as the whole pyrolysis vapor goes directly into the steam reformer.

2.4.4. Steam Reformer

The steam reformer is operated at 850 °C and the ambient pressure with monolith Ni-catalysts. At this temperature, Zhang et al. reported that the coke deposition on the surface of Ni-catalyst could be extensively limited [17]. Monolith catalysts are considered for the process as they can reduce pressure drop, easy to be installed, durable, and able to withstand various conditions [30,41]. Furthermore, a successful application of monolith catalysts for steam reforming has been proved at an industrial scale [41]. As explained before, it should be noted that the addition of a guard bed before the Ni-catalyst bed might be crucial in Scheme 1 due to the heavy fraction of bio-oil which cause rapid catalyst deactivation [30,31].

Table 6. Summary of blocks and streams used in the Aspen Plus model.

Abbreviations	Type of Block	Function
<i>Blocks</i>		
COOL1	Heater	Syngas cooling before being fed to the WGS reactor.
COOL2	Heater	Cooling of the WGS reactor's H ₂ -rich gas products.
COOL3	Heater	An intra-cooling unit for the PSA module.
COMP1	Compressor	Compression of the H ₂ -rich vapor to 1 MPa prior to the PSA module.
COND	Flash2	Bio-oil condenser prior to the reforming process.
DECOMP	RYield	Conversion of the non-conventional bio-oil's high molecular weight lignin fraction to its basic molecules (C, H ₂ , and O ₂). Only for Scheme 1.
HX1	HeatX	Recovering the heat of reformer's syngas to preheat the pyrolysis vapor stream.
HX2	HeatX	Further heat recovery of reformer's syngas to generate steam input for the reforming process.
HX3	HeatX	Generation of WGS steam input by recovering the sensible heat of the WGS outlet stream.
MIX1	Mixer	Mixing of the condensed water and the make-up water.
REFORM	RGibbs	Catalytic steam reforming of pyrolysis vapor at 850 °C.
SEP1	Sep	Separation of pyrolysis vapor stream into a light fraction (conventional) and a high molecular weight lignin fraction (non-conventional).
SEP2	Sep	Condenser to separate water from the H ₂ -rich dry gases.
PSA	Sep	PSA module operated at 1 MPa and 50 °C.
PUMP1	Pump	Water supply to the steam reformer.
PUMP2	Pump	Water supply to the WGS reactor.
WGS	RStoic	WGS reactor operated at 425 °C and ambient pressure.
<i>Streams</i>		
HMWLIG1		The non-conventional bio-oil's high molecular weight lignin fraction.
HMWLIG2		Basic molecules of the non-conventional bio-oil's high molecular weight lignin fraction.
H2		Final H ₂ product from the PSA module.
H2O-COND		Condensed water separated from the WGS reactor product.
H2O-MAKE		Make-up water needed for the co-production system.
H2O-REF1		Water supply for the reforming process.
H2O-REF2		Pumped water supply for the reforming process.
H2O-REF3		Steam input for the reforming process.
H2O-SPLY		Water supply for the entire co-production system.
H2O-WGS1		Water supply for the WGS reactor.
H2O-WGS2		Pumped water supply for the WGS reactor.
H2O-WGS3		Steam input for the WGS reactor.
LIGHT		Separated light fraction of the pyrolysis vapor. Contains all the uncondensed gases and bio-oil compounds except the high molecular weight lignin fraction.
PYRO1		Pyrolysis vapor produced from the biomass pyrolysis. The content of this stream is determined based on the experimental and calculation results.
PYRO2		In Scheme 1: Preheated pyrolysis vapor going into the reformer. In Scheme 2: Uncondensed pyrolysis vapor going into the heat exchanger.
PYRO3		Preheated pyrolysis vapor going into the reformer. Only in Scheme 2.
REST		Contains of mostly CO ₂ with minor fraction of CO and CH ₄ .
VP1		High-temperature syngas (850 °C) produced from the reformer. The stream consists of H ₂ , CO, CO ₂ , and CH ₄ .
VP2		Cooled syngas after heat exchanger "HX1".
VP3		Cooled syngas after heat exchanger "HX2".
VP4		Syngas input for the WGS reactor.
VP5		H ₂ -rich gases produced by the WGS reactor.
VP6		Cooled H ₂ -rich gases.
VP7		Cooled H ₂ -rich gases.
VP8		Dry H ₂ -rich gases.
VP9		Compressed dry H ₂ -rich gases.
VP10		Dry H ₂ -rich gases input for PSA module.

2.4.5. WGS Reactor

Subsequently, the reformer's cooled gas products are fed to a high-temperature (HT) WGS reactor. The flowsheet diagram of the process can be seen in Figure 5. The WGS reactor uses a Fe/Cr-based commercial catalyst that has been successfully tested to produce H_2 from a tar-rich syngas generated from gasification of biomass [42]. The reactor is operated at 425 °C and ambient pressure. A molar steam to dry gas ratio of 1.5 is used to prevent coking and carbon deposition on the catalyst surface [43]. The molar amount of steam fed to the WGS reactor is calculated by writing a FORTRAN code, which is executed before the unit operation ("WGS" block). The code is written in a calculator block based on the following formula,

$$n_{H_2O-WGS} = [1.5 (n_{CO} + n_{CO_2} + n_{CH_4})] - n_{H_2O-syngas} \quad (4)$$

where n_{H_2O-WGS} is the molar rate (kmol/h) of the steam supply needed for the WGS reactor; and n_{CO} , n_{CO_2} , n_{CH_4} , and $n_{H_2O-syngas}$ are the molar rate (kmol/h) of the CO, CO₂, CH₄, and existing steam in the syngas input stream to the WGS reactor, respectively. The HT WGS reactor is simulated using an adiabatic stoichiometric model (RStoic) with a CO conversion rate of 0.92 [42]. The amount of required catalyst for WGS process is calculated based on the gas hourly space velocity (GHSV) constant of 479 h⁻¹ [42]. This constant is determined as the ratio of the volumetric dry gas flow rate at the inlet of the WGS reactor to the catalyst volume.

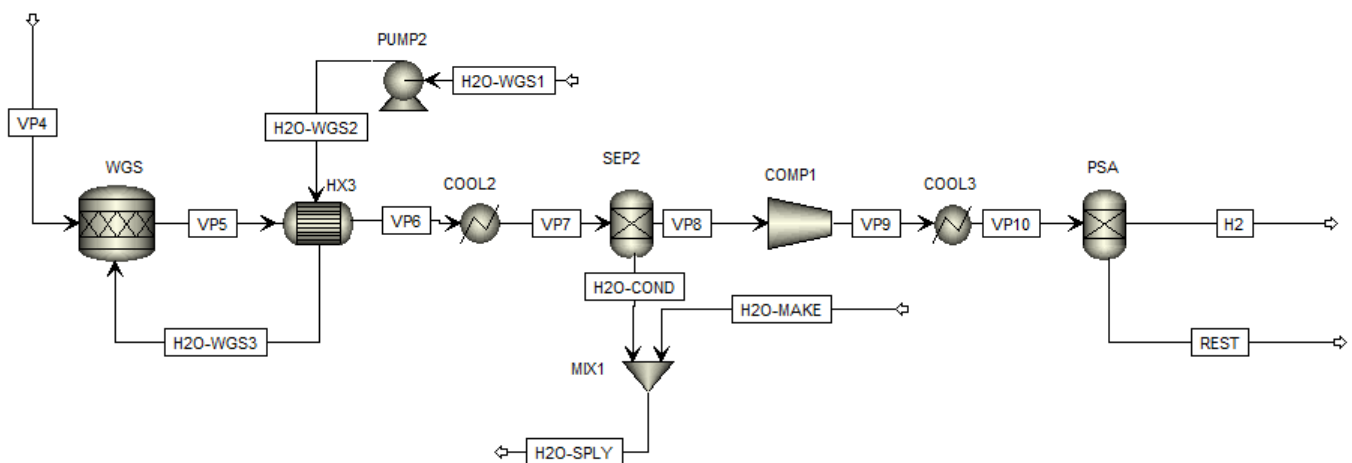


Figure 5. Flowsheet diagram of the WGS and PSA processes.

2.4.6. Pressure Swing Absorber (PSA)

The gas stream produced from the WGS reactor is then cooled to condense the steam fraction. The dried gas is then compressed to 1 MPa and fed to the PSA module operated at 50 °C. In this simulation, the PSA model is simplified using a separator block ("PSA").

2.5. System Evaluation

The performance of the proposed co-production systems is evaluated by using H_2 (η_{H_2}), bio-oil ($\eta_{bio-oil}$), and total thermal (η_{th}) efficiencies which are formulated as follow:

$$\eta_{H_2} = \frac{LHV_{H_2} \cdot \dot{m}_{H_2}}{E_{in}} \quad (5)$$

$$\eta_{bio-oil} = \frac{LHV_{biooil} \cdot \dot{m}_{bio-oil}}{E_{in}} \quad (6)$$

$$\eta_{th} = \frac{LHV_{H_2} \cdot \dot{m}_{H_2} + LHV_{bio-oil} \cdot \dot{m}_{bio-oil} + LHV_{biocarbon} \cdot \dot{m}_{biocarbon}}{E_{in}} \quad (7)$$

$$E_{in} = (LHV_{biomass} \cdot \dot{m}_{biomass}) + W_{pyrolysis} + W_{reformer} + W_{auxiliaries} \quad (8)$$

where $LHV_{biomass}$, LHV_{H_2} , $LHV_{bio-oil}$, and $LHV_{biocarbon}$ are the LHV (kJ/kg) of biomass, H_2 , bio-oil, and biocarbon, respectively; $\dot{m}_{biomass}$, \dot{m}_{H_2} , $\dot{m}_{bio-oil}$, and $\dot{m}_{biocarbon}$ are the mass flow rate (kg/h) of biomass, H_2 , bio-oil, and biocarbon, respectively; $W_{pyrolysis}$ is the electrical power (kW) to heat the pyrolysis reactor, $W_{reformer}$ is the electrical power (kW) to heat the steam reformer, and $W_{auxiliaries}$ is the duties (kW) of compressors and pumps.

3. Results and Discussion

3.1. Mass and Energy Flow

3.1.1. Scheme 1

Figure 6a shows the mass flow diagram of production system Scheme 1, in which biocarbon and H_2 are produced from 1000 kg/h of biomass. In the pyrolysis reactor, the biomass with a moisture content of 7 wt.% can be converted into 217.2 kg of biocarbon. The remaining vapor fraction (782.8 kg/h) is then fed into the steam reforming, where 393.4 of steam is added into the reaction to meet the required S/C ratio. The steam amount in the reformer's outlet stream is insufficient to reach a molar steam to dry gas ratio of 1.5 required for the WGS reactor; hence, 263.1 kg/h of steam is added to the WGS process. At the final stream outlet, 93.5 kg/h of H_2 can be produced or equal to 10.0 wt.% of dry biomass input (see Table 7); while 943.2 kg/h of CO_2 can be separated from the stream which corresponds to 101.1 wt.% of dry biomass.

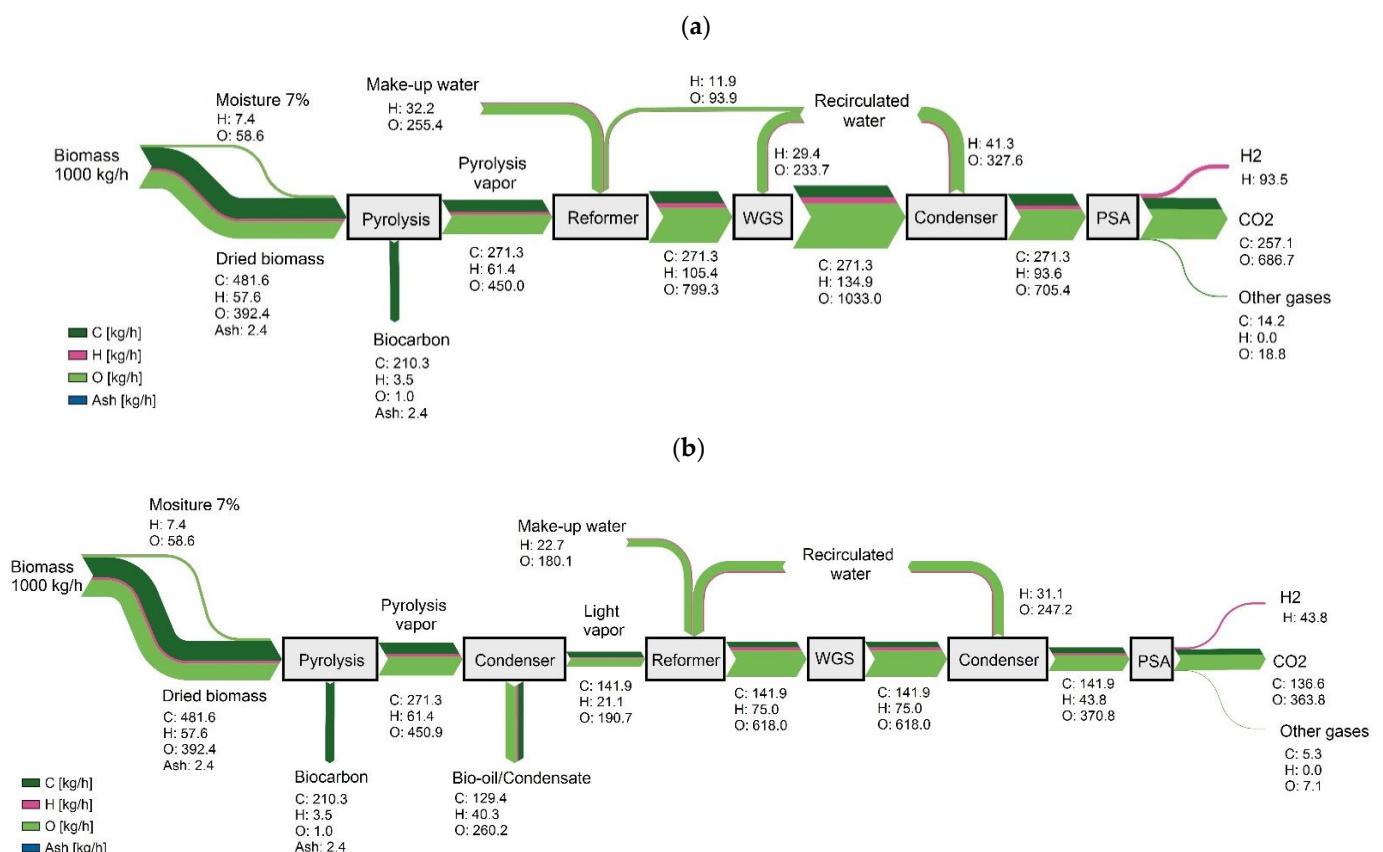


Figure 6. Mass flow diagrams for production scheme of (a) biocarbon and H_2 (scheme 1); and (b) biocarbon, bio-oil, and H_2 with condenser temperature of 50 °C (scheme 2).

Table 7. Product yields and efficiencies of Schemes 1 and 2.

Parameters	Scheme 1	Scheme 2 *
H ₂ yield (wt.% dry biomass)	10.0	4.7
CO ₂ yield (wt.% dry biomass)	101.1	53.6
Bio-oil yield (wt.% dry biomass)	-	46.0
η_{H_2} (%)	47.1	22.9
$\eta_{bio-oil}$ (%)	-	23.1
η_{th} (%)	79.0	79.0

* temperature of the bio-oil condenser at 50 °C.

The energy flow diagram of Scheme 1 is shown in Figure 7a. To operate the pyrolyzer at 550 °C, 420 kW of power is needed as an electrical heating source, which is equal to 1.6 MJ/kg of dry biomass input. This value is in the same range of heat required for pyrolysis of pine of 1.5–1.9 MJ/kg reported in the literature [44,45]. Meanwhile, 699.7 kW of electrical power is required to maintain the steam reformer at 850 °C. The reformer's reactions are endothermic; thus, a significant amount of energy is needed, especially when the reactor is set to a high temperature. On the other hand, no additional energy is needed to operate the WGS reactor as the WGS reaction is exothermic and the heat required to generate steam input can be easily supplied through the heat exchanger (HX3). Overall, the values of η_{H_2} and η_{th} of Scheme 1 are 47.1 and 79.0, respectively.

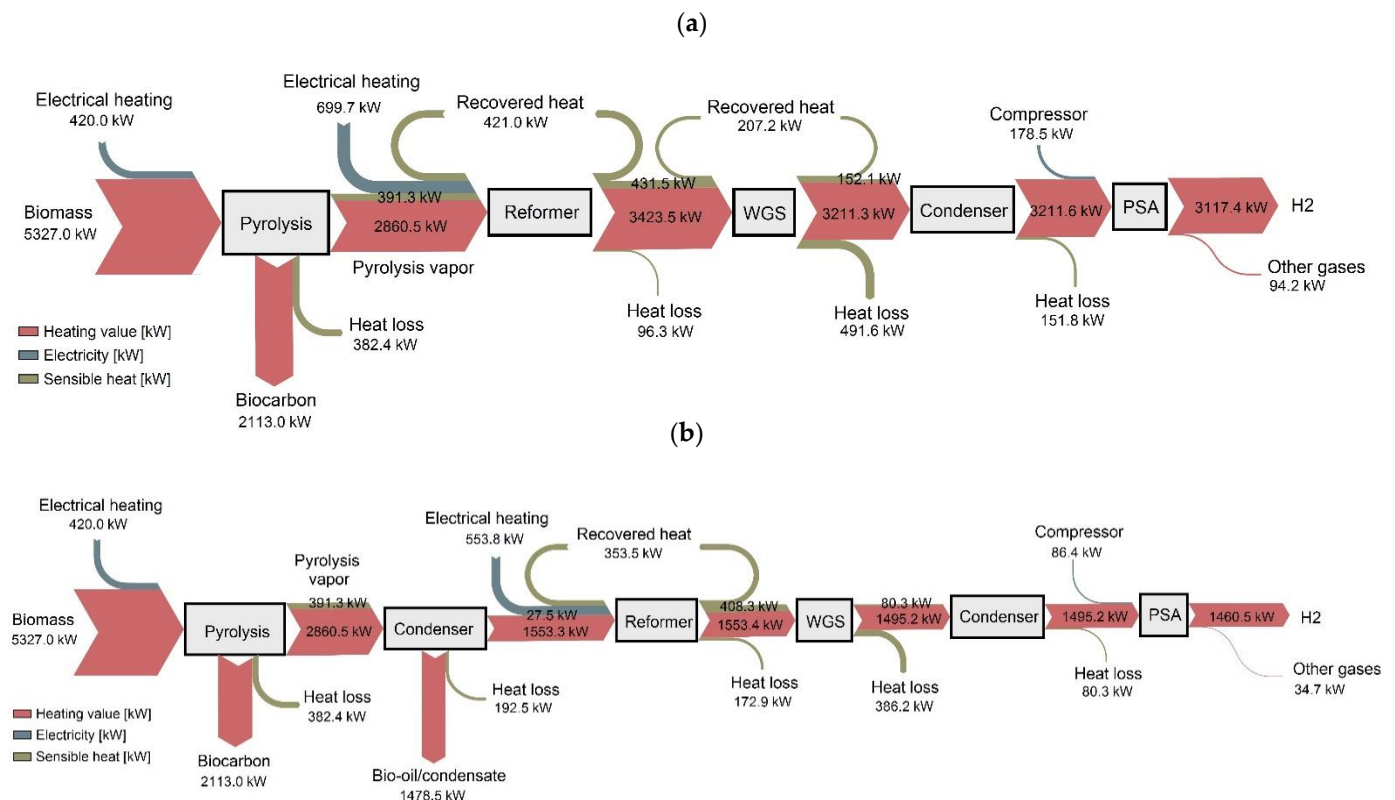


Figure 7. Energy flow diagrams for production scheme of (a) biocarbon and H₂ (Scheme 1); and (b) biocarbon, bio-oil, and H₂ with condenser temperature of 50 °C (Scheme 2).

3.1.2. Scheme 2

Figure 6b shows the mass flow diagram of Scheme 2, in which bio-oil is collected by condensing the pyrolysis vapor at 50 °C. At the condenser, slightly more than half of the pyrolysis vapor weight can be condensed into bio-oil. This result corresponds to approximately 46.0 wt.% of dry biomass flowrate. Nevertheless, the condensed bio-oil's

water content reaches 41.7 wt.%, which cause a relatively low LHV of 5.9 MJ/kg. As the H₂O mostly condense to the bio-oil fraction, the light vapor that goes to the steam reformer contains only dry gases. Thus, a higher amount of additional steam is needed at the reformer's inlet than that of Scheme 1, to satisfy the required S/C ratio. However, no additional steam is required for the WGS reactor as the reformer's syngas contains enough steam. Overall, the system needs a 41.8% lower amount of make-up water than Scheme 1. The final value of H₂ yield is almost half of Scheme 1's value which is approximately 4.7 wt.% dry biomass.

Figure 7b presents the energy flow diagram of Scheme 2. Even though the reforming process needs a higher flow rate of steam, the total heat needed for the process is lower (20.9% lower) than Scheme 1. This is because the amount of pyrolysis vapor stream input is lower compared to Scheme 1. As seen in Figure 6b, stream input's mass flow is 353.7 kg/h, which is 54.8% lower than that of Scheme 1. Accordingly, the reformer requires lower energy to maintain the reaction at 850 °C. Lastly, the production system can achieve η_{H_2} and $\eta_{bio-oil}$ values of 22.9 and 23.1, respectively. Meanwhile, there are not any differences regarding the value of η_{th} , as the value for both systems is 79.0%.

3.2. Sensitivity Analysis

3.2.1. Effect of Temperature of the Bio-Oil Condenser

The temperature of the bio-oil condenser is varied between 50–130 °C to investigate its effect on the system performance of Scheme 2. As seen in Figure 8, changing the condenser temperature obviously affects the product distribution. At 50 °C, the bio-oil yield value is 46.0 wt.% dry biomass which notably decreases with the raise of condenser temperature until 100 °C. At a temperature above 100 °C, no significant reduction can be observed for the bio-oil yield. At the highest temperature of 130 °C, the bio-oil yield is equal to 19.1 wt.% dry biomass. It should be noted that in this simulation, the lumped high MW lignin-derived fraction of bio-oil is assumed as a non-conventional compound which fully condenses within the investigated temperature range. The application of a more accurate model of this compound's condensation characteristics might result in a shifted bio-oil yield.

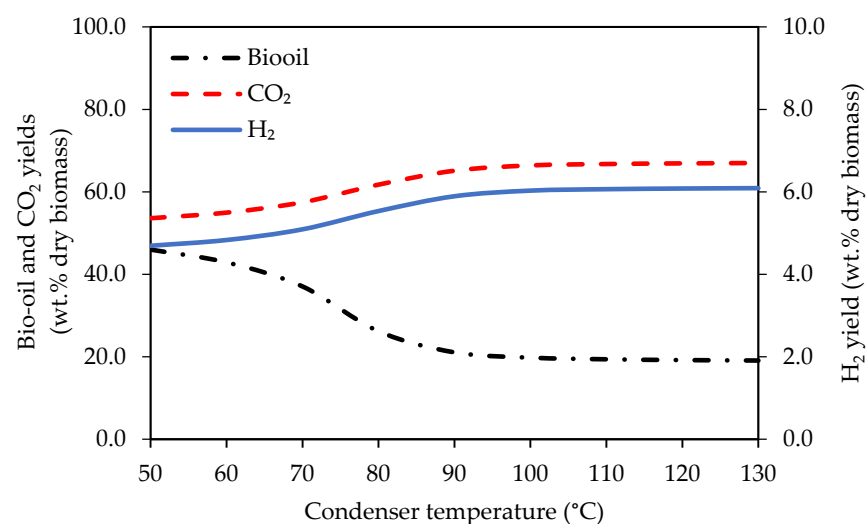


Figure 8. The yield of bio-oil, H₂, and CO₂ obtained from Scheme 2 production system at different bio-oil condenser temperatures.

Figure 9 depicts the LHV and the water content of bio-oil collected from different condenser temperature. More steam can be condensed at a lower condenser temperature, which causes the water content of bio-oil to increase. As seen in the figure, at 50 °C, the bio-oil contains an approximately 41.7 wt.% of water content, while less than 1 wt.% of water content is obtained in the case of 130 °C. The high content of water consequently

causes the bio-oil to have a low LHV. For instance, in the case of 50 °C, the LHV is only 5.9 MJ/kg, which is 27.0% lower than that of 130 °C.

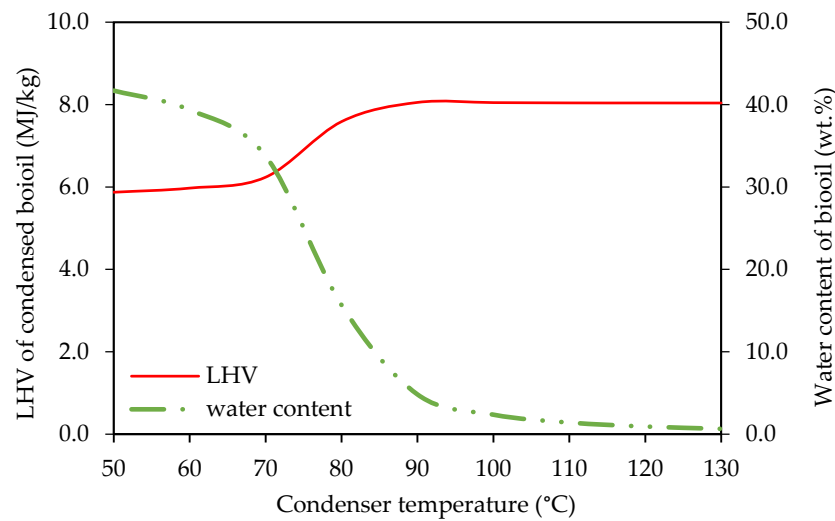


Figure 9. LHV and water content of bio-oil obtained from different condenser temperatures.

Operating the condenser at a different temperature only slightly affects the total thermal efficiency of the system. As seen in Figure 10, at a higher condenser operating temperature, Scheme 2 has a higher η_{th} value. Raising the condenser temperature from 50 to 130 °C results in a merely 1% higher of η_{th} value. This small change is mainly caused by the lower amount of heat loss at the condenser when it set to a higher operating temperature.

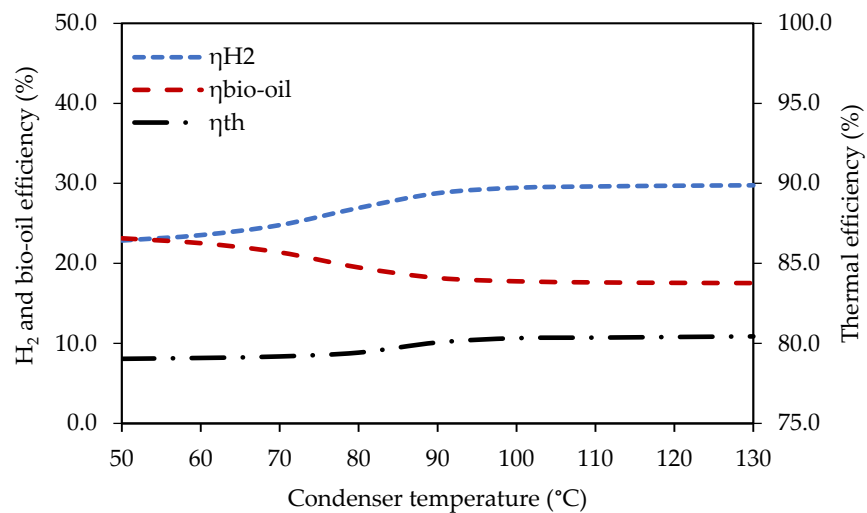


Figure 10. H_2 (η_{H_2}) and total thermal (η_{th}) efficiencies of Scheme 2 production system at different temperatures of the bio-oil condenser.

3.2.2. Effect of Moisture Content of Biomass

Table 8 shows the performance parameters' values of Scheme 2 when the biomass feed has different moisture contents of 7 and 14 wt.%. This sensitivity analysis is performed with the assumption of a condenser temperature of 50 °C. A higher biomass moisture content obviously reduces the system performance of Scheme 2, at which the value of η_{th} decrease from 79.0% to 72.6% as the moisture content increase from 7 to 14 wt.%. The efficiency value decreases mainly due to the reduction of the products' total energy value at lower yield values. For instance, the calorific value of biocarbon, bio-oil, and H_2 are 1945.5, 1361.1, and 1345.3 kW, respectively, when there is a 14 wt.% of moisture content

in biomass. These values are approximately 8% lower than that of 7% biomass moisture content. The H₂ and CO₂ yields do not show different values for both cases regarding the dry weight of biomass, suggesting that the product distribution at the reformer and WGS reactor is similar.

Table 8. Product yields and efficiencies of Scheme 2 with different moisture contents of biomass and bio-oil condenser temperature of 50 °C.

Parameters	Moisture Content of Biomass (wt.%)	
	7	14
H ₂ yield (wt.% dry biomass)	4.7	4.7
CO ₂ yield (wt.% dry biomass)	53.6	53.7
H ₂ yield (wt.% wet biomass)	4.4	4.0
CO ₂ yield (wt.% wet biomass)	50.0	46.1
η_{biooil} (%)	23.1	21.2
η_{H_2} (%)	22.9	21.0
η_{th} (%)	79.0	72.6

3.3. Operating Expense Evaluation

Operating expense (OPEX) is calculated to evaluate the economics of the process partially. The OPEX is calculated for three different cases as follows.

Case 1: In this case, Scheme 1 is used to produce only biocarbon and H₂.

Case 2: In this case, Scheme 2 is used in which the condenser before the steam reformer is operated at a low temperature of 50 °C to collect bio-oil.

Case 3: In this case, Scheme 2 is used in which the condenser before the steam reformer is operated at a high temperature of 130 °C.

Table 9 lists the assumptions for the OPEX calculation. Reformer catalyst is assumed to be a monolith catalyst; therefore, the make-up catalyst is not required. Occasionally every 1–3 months, the monolith catalyst will require regeneration or cleaning [41]. WGS catalyst is assumed to be in the form of pellets. The amount of catalyst load is determined based on the GHSV constant of 479 h⁻¹, which are 3566, 1827, and 2362 kg for Case 1, Case 2, and Case 3, respectively. Table 10 summarizes the main process parameters used in the OPEX calculation. Bio-oil prices in case 2 and 3 are calculated based on water content and dry bio-oil price.

Annual operation costs are shown in Table 11. The feedstock and personnel costs are the main expenses and are same for all cases, while the costs for reformer and WGS vary depending on the amount of vapor going into reformer in each case. Case 1 has the highest operating cost due to the higher amount of vapor going into the reformer. Moreover, Case 1 also has the lowest revenue. This results in Case 1 being the least economical based on operating cost alone. However, the capital cost for Case 1 is expected to be lower than Case 2 and 3 because a bio-oil condenser is not required in Case 1. Another operational cost not considered is the reformer catalyst regeneration cost which is expected to be higher in Case 1 due to the larger volume of the pyrolysis vapor needed to be reformed.

The loss/gain based on OPEX without considering CO₂ as a commodity suggests that the most economical process is Case 2 with the gain of 0.31 SEK/kg-biomass fed. This assumes that the bio-oil with high water content could be sold without further processing.

When considering CO₂ as a commodity, the total revenue doubles in Case 2 and 3, and increases four times in Case 1. The loss/gain based on OPEX is then positive for all cases with more than 10 SEK/kg of biomass. Nevertheless, CO₂ is not usually considered a commodity but as an emission that could arguably be carbon neutral.

Table 9. The assumption for the OPEX calculation.

Parameter	Assumption	References
Duration of operation	8000 h/yr	
Raw materials		
Biomass pellet	6.6 wt.% moisture content	
Reformer catalyst	3 SEK/kg Monolith catalyst	Retail price [46] [41]
WGS catalyst	No make-up catalyst required 0.215 SEK/kg	[27]
Solid disposal (spent catalyst)	0.02 wt.% hourly make-up 3.9 SEK/kg	[47]
Products		
H ₂	33 SEK/kg	[48]
Biocarbon	8 SEK/kg	Envigas
Bio-oil crude	9 SEK/kg dry oil	Envigas
CO ₂	11.1	Retail price [49]
Utilities		
Electricity	0.7 SEK/kWh	[50]
Water	9.75 SEK/m ³	
Personnel		
Plant manager (1 person)	70,000 SEK/person/month	
Plant engineer (1 person)	50,000 SEK/person/month	
Shift operators (12 person)	30,000 SEK/person/month	
Overheads	90% of total salaries	

Table 10. Summary of the main process parameters for OPEX calculation.

Parameter	Case 1	Case 2	Case 3
Pyrolysis			
Biomass pellet (kg/h)	1000	1000	1000
Reactor heating (kW)	420.3	420.3	420.3
Bio-oil condenser			
Recirculation pump (kW)	-	7.5	7.5
Reformer			
Reactor heating (kW)	699.70	553.80	464.30
Water supply (kg/h)	287.60	350.57	202.88
WGS reactor			
Make-up catalyst (kg/h)	0.71	0.37	0.47
Water supply (kg/h)	0.00	0.00	0.00
Solid disposal (kg/h)	0.71	0.37	0.47
PSA			
Compressor and utilities (kW)	178.50	86.40	111.10
Products yields			
Biocarbon (kg/h)	217.20	217.20	217.20
H ₂ (kg/h)	93.55	43.83	57.00
Bio-oil (kg/h)	0.00	429.69	178.15
CO ₂ (kg/h)	944.39	500.32	628.18
Bio-oil price			
Water content in bio-oil (wt.%)		41.70%	0.64%
Bio-oil price based on water content	-	5.25	8.94

Table 11. Annual operation costs for the co-production process of biocarbon, hydrogen, and bio-oil.

Parameter	Case 1	Case 2	Case 3
Variable operating cost (MSEK/year)			
Pyrolysis			
Biomass pellet	24.00	24.00	24.00
Reactor heating	2.35	2.35	2.35
Bio-oil condenser			
Recirculation pump	-	0.04	0.04
Reformer			
Reactor heating	3.92	3.10	2.60
Water supply	0.02	0.03	0.02
WGS reactor			
Make-up catalyst	0.001	0.001	0.001
Solid disposal	0.022	0.011	0.015
PSA			
Compressor and utilities	1.00	0.48	0.62
Fixed operating cost (MSEK/year)			
Salary	5.76	5.76	5.76
Overhead	5.184	5.184	5.184
Products values (MSEK/year)			
Biocarbon	13.90	13.90	13.90
H ₂	24.70	11.57	15.05
Bio-oil	0.00	17.19	12.83
CO ₂	83.86	44.43	55.78
Total OPEX (MSEK/year)	42.26	40.96	40.59
Total revenue (MSEK/year)	38.60	42.66	41.78
Total revenue including CO ₂ (MSEK/year)	122.46	87.09	97.56
Gross production cost¹ (SEK/kg-biomass)	5.28	5.12	5.07
Loss/Gain based on OPEX² (SEK/kg-biomass)	-0.46	0.32	0.14
Loss/Gain based on OPEX ² with CO ₂ (SEK/kg-biomass)	23.85	13.97	16.92
Minimum biocarbon selling price³ (SEK/kg)	10.11		
Minimum bio-oil selling price⁴ (SEK/kg)		3.44	5.59

¹ Gross production cost = Total OPEX/kg-biomass fed. ² Loss/Gain based on OPEX = (Total revenue—Total OPEX)/kg-biomass fed. ³ Not including capital investment. ⁴ Not including capital investment. In addition, using the same biocarbon price as case 1.

A minimum biocarbon selling price for Case 1 is calculated based on the biocarbon price that gives zero loss/gain based on OPEX alone. The value is 10.11 SEK/kg, which is comparable to retail prices for grill charcoal in Sweden of 12–35 SEK/kg [51]. It is also comparable to the price of coking coal, which is around 10–20 SEK/kg, while coal's commercial price is 5–10 SEK/kg [52].

The minimum biocarbon selling price for Case 1 was used in Case 2 and 3 to calculate the minimum selling price for bio-oil. It was found that the prices are 3.44 and 5.59 SEK/kg, respectively. The bio-oil price for Case 3 is comparable to that of crude oil. Nevertheless, the application of bio-oil in existing refinery still needs more study and testing. An initiative to refine bio-oil on an industrial scale is on-going in Sweden [53]. For bio-oil with high water content as in Case 2 with 41.7 wt.% water, post-processing is needed to reduce water content or fractionate the oil. Fermentation is another pathway to use high water content bio-oil [54].

Although Case 2 is the most economical cases based on OPEX, there is still some future consideration that might hinder this process's economics. First, Case 2 (and 3) requires capital investment for a condenser. Second, Case 2 compared to Case 3 requires post-processing of bio-oil due to the high water content.

4. Conclusions

In this study, two different co-production schemes of H₂, biocarbon, and bio-oil are proposed based on the 1000 kg/h biomass pyrolysis plant available at Envigas, Sweden. Two production schemes are proposed: (1) to produce biocarbon and H₂ and (2) to produce biocarbon, H₂ and bio-oil. Process simulations using Aspen Plus were carried out to assess those schemes under different operating parameters. The results indicate that both Scheme 1 and Scheme 2 exhibit a similar value of total thermal efficiency despite their different H₂ and bio-oil yields. Varying the bio-oil condenser temperature only slightly changes the system's thermal efficiency by less than 2%. On the other hand, an increase in biomass moisture content from 7 to 14 wt.% can decrease the system's efficiency from 79.0 to 72.6%.

Furthermore, operating expense is evaluated to clarify the economics of 3 different cases which are (1) no bio-oil production, (2) bio-oil production with the condenser at 50 °C, and (3) bio-oil production with the condenser at 130 °C. Based on OPEX and revenue alone, it is found that producing more bio-oil can improve the economic feasibility of the process. However, capital costs and the cost for post-processing of bio-oil should also be considered in the future. The estimated minimum selling price for biocarbon based on only OPEX is approximately 10 SEK, which is within a price range of commercial charcoal and coke in Sweden.

Author Contributions: Conceptualization, all; methodology, I.N.Z. and N.S.; software, I.N.Z.; validation, all; formal analysis, I.N.Z. and N.S.; investigation, I.N.Z. and N.S.; resources, K.S. and W.Y.; writing—original draft preparation, I.N.Z. and N.S.; writing—review and editing, all; visualization, I.N.Z. and N.S.; supervision, K.S. and W.Y.; funding acquisition, K.S. and W.Y. All authors have read and agreed to the published version of the manuscript.

Funding: This research received financial supports from the Swedish Energy Agency (Energimyndigheten).

Institutional Review Board Statement: Not applicable.

Informed Consent Statement: Not applicable.

Data Availability Statement: Not applicable.

Acknowledgments: N.S. would like to thank DPST project, Thailand, for mental support.

Conflicts of Interest: The authors declare no conflict of interest. The funders had no role in the design of the study; in the collection, analyses, or interpretation of data; in the writing of the manuscript, or in the decision to publish the results.

References

1. Sveriges Geologiska Undersökning (SGU) Bergverksstatistik 2019: Statistics of the Swedish Mining Industry. 2019. Available online: <http://resource.sgu.se/bergsstaten/bergverksstatistik-2019.pdf> (accessed on 11 November 2020).
2. Sandberg, H.; Lagneborg, R.; Lindblad, B.; Axelsson, H.; Bentell, L. CO₂ emissions of the Swedish steel industry. *Scand. J. Metall.* **2001**, *30*, 420–425. [CrossRef]
3. Suopajarvi, H.; Umeki, K.; Mousa, E.; Hedayati, A.; Romar, H.; Kempainen, A.; Wang, C.; Phounglamcheik, A.; Tuomikoski, S.; Norberg, N.; et al. Use of biomass in integrated steelmaking—Status quo, future needs and comparison to other low-CO₂ steel production technologies. *Appl. Energy* **2018**, *213*, 384–407. [CrossRef]
4. Babich, A.; Senk, D. Coke in the iron and steel industry. In *New Trends in Coal Conversion*; Elsevier: Amsterdam, The Netherlands, 2019; pp. 367–404.
5. Pei, M.; Petäjäniemi, M.; Regnell, A.; Wijk, O. Toward a fossil free future with hybrit: Development of iron and steelmaking technology in Sweden and Finland. *Metals* **2020**, *10*, 972. [CrossRef]
6. Mousa, E.; Wang, C.; Riesbeck, J.; Larsson, M. Biomass applications in iron and steel industry: An overview of challenges and opportunities. *Renew. Sustain. Energy Rev.* **2016**, *65*, 1247–1266. [CrossRef]
7. Sveaskog Brief Facts 1: What is Swedish Forestry? Available online: <https://www.sveaskog.se/en/forestry-the-swedish-way/short-facts/brief-facts-1/> (accessed on 26 January 2021).
8. Swedish Bioenergy Assn (Svebio). Roadmap Bioenergy—Meeting the Demand for Bioenergy in a Fossil Free SWEDEN. 2020. Available online: <https://www.svebio.se/app/uploads/2020/03/Roadmap-Bioenergy-2020.pdf> (accessed on 26 January 2021).

9. Phounglamcheik, A.; Wang, L.; Romar, H.; Kienzl, N.; Broström, M.; Ramser, K.; Skreiberg, Ø.; Umeki, K. Effects of Pyrolysis Conditions and Feedstocks on the Properties and Gasification Reactivity of Charcoal from Woodchips. *Energy Fuels* **2020**, *34*, 8353–8365. [CrossRef]
10. Sophonrat, N.; Brink, T.; Sjöblom, K. PyNe 45 Newsletter—IEA Bioenergy Task 34. 2019, pp. 13–17. Available online: https://task34.ieabioenergy.com/wp-content/uploads/sites/3/2019/12/PyNe-45_final.pdf (accessed on 30 November 2020).
11. Arregi, A.; Amutio, M.; Lopez, G.; Bilbao, J.; Olazar, M. Evaluation of thermochemical routes for hydrogen production from biomass: A review. *Energy Convers. Manag.* **2018**, *165*, 696–719. [CrossRef]
12. Shiva Kumar, S.; Himabindu, V. Hydrogen production by PEM water electrolysis—A review. *Mater. Sci. Energy Technol.* **2019**, *2*, 442–454. [CrossRef]
13. Zaini, I.N.; Nurdiawati, A.; Aziz, M. Cogeneration of power and H₂ by steam gasification and syngas chemical looping of macroalgae. *Appl. Energy* **2017**, *207*, 134–145. [CrossRef]
14. Zaini, I.N.; Gomez-Rueda, Y.; García López, C.; Ratnasari, D.K.; Helsen, L.; Pretz, T.; Jönsson, P.G.; Yang, W. Production of H₂-rich syngas from excavated landfill waste through steam co-gasification with biochar. *Energy* **2020**, *207*, 118208. [CrossRef]
15. Nurdiawati, A.; Zaini, I.N.; Irhamna, A.R.; Sasongko, D.; Aziz, M. Novel configuration of supercritical water gasification and chemical looping for highly-efficient hydrogen production from microalgae. *Renew. Sustain. Energy Rev.* **2019**, *112*, 369–381. [CrossRef]
16. Czernik, S.; Evans, R.; French, R. Hydrogen from biomass-production by steam reforming of biomass pyrolysis oil. *Catal. Today* **2007**, *129*, 265–268. [CrossRef]
17. Zhang, S.P.; Li, X.J.; Li, Q.Y.; Xu, Q.L.; Yan, Y.J. Hydrogen production from the aqueous phase derived from fast pyrolysis of biomass. *J. Anal. Appl. Pyrolysis* **2011**, *92*, 158–163. [CrossRef]
18. Norouzi, O.; Jafarian, S.; Safari, F.; Tavasoli, A.; Nejati, B. Promotion of hydrogen-rich gas and phenolic-rich bio-oil production from green macroalgae *Cladophora glomerata* via pyrolysis over its bio-char. *Bioresour. Technol.* **2016**, *219*, 643–651. [CrossRef] [PubMed]
19. Adrados, A.; Lopez-Urionabarrenechea, A.; Solar, J.; Requies, J.; De Marco, I.; Cambra, J.F. Upgrading of pyrolysis vapours from biomass carbonization. *J. Anal. Appl. Pyrolysis* **2013**, *103*, 293–299. [CrossRef]
20. Adrados, A.; Lopez-Urionabarrenechea, A.; Acha, E.; Solar, J.; Caballero, B.M.; de Marco, I. Hydrogen rich reducing gases generation in the production of charcoal from woody biomass carbonization. *Energy Convers. Manag.* **2017**, *148*, 352–359. [CrossRef]
21. Arregi, A.; Lopez, G.; Amutio, M.; Barbarias, I.; Bilbao, J.; Olazar, M. Hydrogen production from biomass by continuous fast pyrolysis and in-line steam reforming. *RSC Adv.* **2016**, *6*, 25975–25985. [CrossRef]
22. Chen, F.; Wu, C.; Dong, L.; Vassallo, A.; Williams, P.T.; Huang, J. Characteristics and catalytic properties of Ni/CaAlO_x catalyst for hydrogen-enriched syngas production from pyrolysis-steam reforming of biomass sawdust. *Appl. Catal. B Environ.* **2016**, *183*, 168–175. [CrossRef]
23. Efika, C.E.; Wu, C.; Williams, P.T. Syngas production from pyrolysis-catalytic steam reforming of waste biomass in a continuous screw kiln reactor. *J. Anal. Appl. Pyrolysis* **2012**, *95*, 87–94. [CrossRef]
24. Xiao, X.; Meng, X.; Le, D.D.; Takarada, T. Two-stage steam gasification of waste biomass in fluidized bed at low temperature: Parametric investigations and performance optimization. *Bioresour. Technol.* **2011**, *102*, 1975–1981. [CrossRef]
25. Ochoa, A.; Arregi, A.; Amutio, M.; Gayubo, A.G.; Olazar, M.; Bilbao, J.; Castaño, P. Coking and sintering progress of a Ni supported catalyst in the steam reforming of biomass pyrolysis volatiles. *Appl. Catal. B Environ.* **2018**, *233*, 289–300. [CrossRef]
26. Situmorang, Y.A.; Zhao, Z.; An, P.; Yu, T.; Rizkiana, J.; Abudula, A.; Guan, G. A novel system of biomass-based hydrogen production by combining steam bio-oil reforming and chemical looping process. *Appl. Energy* **2020**, *268*, 115122. [CrossRef]
27. Jones, S.; Meyer, P.; Snowden-Swan, L.; Susanne, K.J.; Pimphan, M.; Asanga, P.; Eric, T.; Abhijit, D.; Jacob, J. Process Design and Economics for the Conversion of Lignocellulosic Biomass to Hydrocarbon Fuels: Fast Pyrolysis and Hydrotreating Bio-Oil Pathway. U.S. Department of Energy Bioenergy Technologies Office. 2013. Available online: <https://www.nrel.gov/docs/fy14osti/61178.pdf> (accessed on 1 May 2020).
28. Larsson, M.; Görling, M.; Grönkvist, S.; Alvfors, P. Bio-methane upgrading of pyrolysis gas from charcoal production. *Sustain. Energy Technol. Assess.* **2013**, *3*, 66–73. [CrossRef]
29. Arregi, A.; Lopez, G.; Amutio, M.; Artetxe, M.; Barbarias, I.; Bilbao, J.; Olazar, M. Role of operating conditions in the catalyst deactivation in the in-line steam reforming of volatiles from biomass fast pyrolysis. *Fuel* **2018**, *216*, 233–244. [CrossRef]
30. Lónyi, F.; Valyon, J.; Someus, E.; Hancsók, J. Steam reforming of bio-oil from pyrolysis of MBM over particulate and monolith supported Ni/ γ -Al₂O₃ catalysts. *Fuel* **2013**, *112*, 23–30. [CrossRef]
31. Wu, C.; Huang, Q.; Sui, M.; Yan, Y.; Wang, F. Hydrogen production via catalytic steam reforming of fast pyrolysis bio-oil in a two-stage fixed bed reactor system. *Fuel Process. Technol.* **2008**, *89*, 1306–1316. [CrossRef]
32. Wang, D.; Czernik, S.; Montané, D.; Mann, M.; Chornet, E. Biomass to Hydrogen via Fast Pyrolysis and Catalytic Steam Reforming of the Pyrolysis Oil or Its Fractions. *Ind. Eng. Chem. Res.* **1997**, *36*, 1507–1518. [CrossRef]
33. Remiro, A.; Valle, B.; Aguayo, A.T.; Bilbao, J.; Gayubo, A.G. Steam reforming of raw bio-oil in a fluidized bed reactor with prior separation of pyrolytic lignin. *Energy Fuels* **2013**, *27*, 7549–7559. [CrossRef]
34. Guo, W.; Lim, C.J.; Bi, X.; Sokhansanj, S.; Melin, S. Determination of effective thermal conductivity and specific heat capacity of wood pellets. *Fuel* **2013**, *103*, 347–355. [CrossRef]

35. Haseli, Y.; Van Oijen, J.A.; De Goey, L.P.H. Modeling biomass particle pyrolysis with temperature-dependent heat of reactions. *J. Anal. Appl. Pyrolysis* **2011**, *90*, 140–154. [CrossRef]
36. Nurdiawati, A.; Zaini, I.N.; Amin, M.; Sasongko, D.; Aziz, M. Microalgae-based coproduction of ammonia and power employing chemical looping process. *Chem. Eng. Res. Des.* **2019**, *146*, 311–323. [CrossRef]
37. Pinheiro Pires, A.P.; Arauzo, J.; Fonts, I.; Domine, M.E.; Fernández Arroyo, A.; Garcia-Perez, M.E.; Montoya, J.; Chejne, F.; Pfromm, P.; Garcia-Perez, M. Challenges and opportunities for bio-oil refining: A review. *Energy Fuels* **2019**, *33*, 4683–4720. [CrossRef]
38. Li, B.; Lv, W.; Zhang, Q.; Wang, T.; Ma, L. Pyrolysis and catalytic upgrading of pine wood in a combination of auger reactor and fixed bed. *Fuel* **2014**, *129*, 61–67. [CrossRef]
39. Ningbo, G.; Baoling, L.; Aimin, L.; Juanjuan, L. Continuous pyrolysis of pine sawdust at different pyrolysis temperatures and solid residence times. *J. Anal. Appl. Pyrolysis* **2015**, *114*, 155–162. [CrossRef]
40. Goteti, A. Experimental Investigation and Systems Modeling of Fractional Catalytic Pyrolysis of Pine. Ph.D. Dissertation, Georgia Institute of Technology, Atlanta, GA, USA, 2010; p. 218.
41. Voss, B.; Madsen, J.; Hansen, J.B.; Andersson, K.J. Topsøe Tar Reforming in Skive—The tough get going. *Catal. Rev.* **2016**, *29*, 7–14.
42. Kraussler, M.; Binder, M.; Hofbauer, H. 2250-H Long Term Operation of a Water Gas Shift Pilot Plant Processing Tar-Rich Product Gas From an Industrial Scale Dual Fluidized Bed Biomass Steam Gasification Plant. *Int. J. Hydrogen Energy* **2016**, *41*, 6247–6258. [CrossRef]
43. Yao, J.; Kraussler, M.; Benedikt, F.; Hofbauer, H. Techno-economic assessment of hydrogen production based on dual fluidized bed biomass steam gasification, biogas steam reforming, and alkaline water electrolysis processes. *Energy Convers. Manag.* **2017**, *145*, 278–292. [CrossRef]
44. Nugrahany, F. Modelling of Biomass Pyrolysis with Ex-situ Catalytic Upgrading for Bio-crude Production. Master's Thesis, KTH Royal Institute of Technology, Stockholm, Sweden, 2018.
45. Yang, H.; Kudo, S.; Kuo, H.P.; Norinaga, K.; Mori, A.; Mašek, O.; Hayashi, J.I. Estimation of enthalpy of bio-oil vapor and heat required for pyrolysis of biomass. *Energy Fuels* **2013**, *27*, 2675–2686. [CrossRef]
46. Storaenso Köp Pellets i Bulk. Available online: https://www.storaenso.com/sv-se/products/pellets/pellets-for-residential-heating/buy-pellets-bulk?gclid=Cj0KCQjw-O35BRDVARIsAJU5mQWPi4PVUc_o2b5eQWinuRbbl7q-kiDdlMGuMGIG_g3Yo9QKJ-WOSkoaAndNEALw_wcB (accessed on 29 November 2020).
47. Avfall Sverige. Swedish Waste Management 2018. 2018. Available online: https://www.avfallsverige.se/fileadmin/user_upload/Publikationer/Avfallshantering_2018_EN.pdf (accessed on 29 November 2020).
48. Glenk, G.; Reichelstein, S. Economics of converting renewable power to hydrogen. *Nat. Energy* **2019**, *4*, 216–222. [CrossRef]
49. BOC Industrial Gases Price List (ex. VAT). 1 January 2020. Available online: https://www.boconline.co.uk/en/images/industrial-gases-price-list-uk_tcm410-512096.pdf (accessed on 29 November 2020).
50. Sönnichsen, N. Prices of Electricity for Industry in Sweden from 1996 to 2018. Available online: <https://www.statista.com/statistics/596262/electricity-industry-price-sweden/> (accessed on 29 November 2020).
51. Prisjakt Grillkol—Grilltillbehör. Available online: <https://www.prisjakt.nu/c/grilltillbehor?98091=31484> (accessed on 5 January 2021).
52. IEA Coal 2020 Analysis and Forecast to 2025. Available online: <https://www.iea.org/reports/coal-2020/prices-and-costs> (accessed on 5 January 2021).
53. Setra Pyrocell. Available online: <http://www.setragroup.com/en/pyrocell/> (accessed on 5 January 2021).
54. Jarboe, L.R.; Wen, Z.; Choi, D.; Brown, R.C. Hybrid thermochemical processing: Fermentation of pyrolysis-derived bio-oil. *Appl. Microbiol. Biotechnol.* **2011**, *91*, 1519–1523. [CrossRef]